Controlled Pore Generation in Single-Layer Graphene Oxide for Membrane Desalination

Controlled Pore Generation in Single Layer Graphene Oxide for Membrane Desalination

Federico Raffone,* Filippo Savazzi, and Giancarlo Cicero

Dipartimento di Scienza Applicata e Tecnologia, Politecnico di Torino, Corso Duca degli Abruzzi 24, Torino 10129, Italy

E-mail: federico.raffone@polito.it

Abstract

Nanoporous graphene was proposed as an efficient material for reverse osmosis water desalination membranes as it allows water molecules to pass at high fluxes while rejecting hydrated salt ions. Nevertheless, from an experimental point of view it is still difficult to control the pore size. A scalable method to generate pores is urgently required for the diffusion of this technology. We propose, by theoretical calculations, an innovative and scalable strategy to better control the dimension of the pores in graphene-based membranes by reduction of a single layer graphene oxide (GO). The latter is first annealed at a controlled mild temperature to induce the aggregation of its randomly distributed oxygen containing functional groups into small nanometric clusters. The layer then undergoes a high temperature reducing treatment that causes the desorption of the functional groups along with carbon removal only in the oxidized areas producing sub-nanometric pores while leaving unchanged the remaining pristine graphene areas.

Graphical TOC Entry

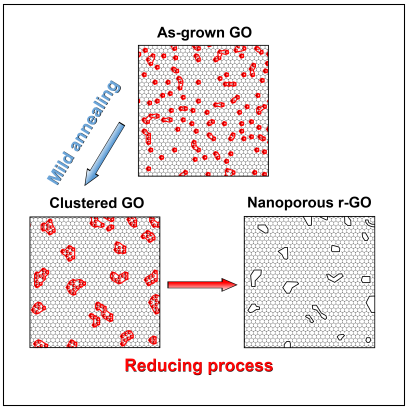

Reverse osmosis plants for water desalination are eager for more selective, as well as more permeable, membranes to reduce the huge energy consumption that afflicts such a technology.[1] Nanoporous graphene membranes can, in principle, constitute an efficient solution for this problem. As first suggested by a computational study,[2] subnanometer pores can filter up to 100% of salt while allowing water to quickly pass. Salt rejection is due to steric effects. Salt ions are surrounded by electrostatically bound water molecules forming a hydration shell that shields the ions charge. The effective volume of the hydration shell is larger than the volume of a single water molecule which, in turn, can readily pass through subnanometer pores. Additionally, graphene membrane permeability overcomes by orders of magnitudes the one of the commercial membranes thanks to its small thickness.[2,3] The increased permeability results in a significant energy saving for desalination plant,[4] making graphene an extremely cost-efficient candidate for filtration. However, for graphene membranes to be applied in reverse osmosis desalination, a reliable control of the pore dimensions must be achieved as even a single over-sized pore can dramatically compromise the selectivity of the membrane. Several techniques were proposed in literature to generate pores. Some of them rely on electron[5] and ion bombardment with heavy ions such as Au[6] or noble gases like Ar[7] which are used to knock-off carbon atoms from the sheet creating holes in graphene. Other methods rely on O_2 plasma,[8] UV or ozone treatment.[9] The produced pores range from fractions of nanometers to tens of nanometers or more. Additionally, molecular dynamics simulations proved that by tilting the focused beam it is possible to tune the geometry of the pores.[10] Although these techniques yield pores of the required dimensions, they are poorly scalable because of the equipment employed to generate the beam and because of the small area of the beam spot size. A theoretical work suggested that if a graphene oxide (GO) monolayer is exposed to high temperatures, the desorption of oxygen containing functional groups (mainly epoxides, ethers and hydroxyls)[11] can cause some carbons to be extracted from the sheet leading to the formation of holes.[12] However, because of the random distribution of the functional groups in GO, with such a thermal reducing process it is not possible

to easily control the size of the pores. Still a proper scalable method to tune the porosity and the selectivity of the graphene-based membrane is missing. Such a lack of approaches to create nanoporous graphene suited for industry is preventing the diffusion of the technology outside the laboratories. It is then of paramount importance for its application to devise other effective and viable processes.

In this work, we propose a new strategy for the precise generation of pores in graphene. The method starts from a single layer graphene oxide used as intermediate to obtain nanoporous graphene membranes. It exploits the natural propensity of GO functional groups to cluster over time. As stated in literature, after synthesis, GO is in a metastable form,[13,14] with functional groups randomly distributed. If the sheet is annealed at mild temperatures (320-350 K) for days, extensive regions of pristine graphene alternated with large oxidized areas appear. The process is said to be driven by a thermally activated diffusion of oxygens. We studied the clusterization process to show how it is influenced by the annealing temperature and the initial oxygen content. We show that, before the formation of two large distinct regions (pristine and oxidized), graphene passes through intermediate states where the mean diameter of the oxidized areas progressively increases. Since the clusterization is found to be a slow process, it can be easily stopped when the diameter of the oxidized areas is on the order of one nanometer. The metastable sheet must then be treated at high temperature (reducing conditions). We prove that only the oxidized areas lead to the formation of pores in the sheet while the perfect graphene areas remain unaltered owing to the stability of the conjugated C=C network. The pores dimension is consistent with the size of the oxidized area. Therefore, by controlling the duration of the mild thermal process it is possible to tune the pore size.

The decisive effect of the clusterization process in the formation of pores was proven by a theoretical modeling. The first part of the work was devoted to provide a quantitative and nanoscopic description of the clustering process. By means of the Cluster Expansion (CE) method coupled with Density Functional Theory (DFT) simulations, it is possible to identify

the energy of all the functional groups arrangements in graphene oxide. This information was then used in Kinetic Monte Carlo (KMC) simulations to describe the evolution of a GO system over time, catching the tendency of the chemical groups to cluster and determining what are the most suitable conditions for the formation of nanometer size oxidized areas. In the second part of the work, we simulated the effects of a strong thermal reducing process on the clustered graphene oxide by means of classical molecular dynamics (MD) heating the GO samples with oxidized clustered areas obtained by KMC.

To model the clusterization process, we first evaluated how the energy of a GO monolayer varies according to the arrangement of the oxygen containing functional groups. For our purpose, monolayer GO can be either synthesized by soft oxidation of graphene[15] without damaging the layer or through non-destructive exfoliation of multilayer GO[16–18] In as-grown GO layers the groups are randomly distributed but occupy well defined positions: bridge between two carbons for the epoxides/ethers and on top of a carbon atom for the hydroxyls as shown in Fig. 1a-c.

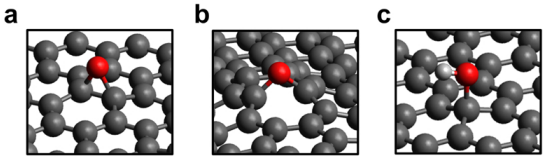

Figure 1: Representation of the functional groups adsorbed on graphene: epoxides (a), ethers (b) and hydroxyls (c). Carbon atoms are depicted in gray, oxygens in red and hydrogens in white.

GO samples with different functional group arrangement have different total energies. This can be predicted by CE, a technique able to provide the energy of a system existing in several configurations. In CE a material is thought to be made of a grid of sites that can be occupied by either one species or another. For such a reason, CE was applied to alloys[19–21] for which the full concentration range is relevant. However, lately CE was employed in the low coverage range to study surface chemisorptions[22–24] ensuring the reliability of the method in describing -OH and -O- covered graphene. In our simulations we neglected hydroxyls

and we treated only epoxides and ethers, as they are reported to be the most relevant species to generate pores by thermal reduction because of the large strain induced in the sheet.[11,12] Moreover, both calculations and experiments suggest that the diffusion of epoxides and hydroxyls tend to segregate into distinct domains containing only epoxides or only hydroxyls.[25,26] Experimentally it is also possible to obtain GO containing only epoxide or hydroxyl groups.[27–30] Unlike CE for alloys, in graphene each site of the grid can be either occupied or unoccupied by an epoxide (bridge on two nearest neighbour carbon atoms). According to CE, the energy of a configuration is given by the sum of the decomposed energetic contributions of the clusters constituting a configuration $\boldsymbol{\sigma}$. For the sake of clarity, we will refer to them as "figures" rather than clusters in order to avoid confusion with the clustering process resulting from the grouping of epoxides on the GO layer. A figure represents a set of sites on the grid. It can vary in number of combined sites (1 for singlets, 2 for pairs, 3 for triplets and so forth up to infinity) and maximum distance among sites. Each figure is given by the product of occupancy variables σ which take the value of 1 or 0, following the lattice-gas Hamiltonian convention,[31] whether the site is occupied or not. The impact of each figure on the total energy is given by the Effective Cluster Interactions J (ECI). Formally, the configurational energy can be written in the lattice-gas Hamiltonian convention as:

$$H(\boldsymbol{\sigma}) = H_0 + \sum_{i=1}^{S_L} h_i\sigma_i + \sum_{i=1}^{S_L}\sum_{j=i+1}^{S_L} J_{ij}\sigma_i\sigma_j + \\ + \sum_{i=1}^{S_L}\sum_{j>i}^{S_L}\sum_{k>j}^{S_L} J_{ijk}\sigma_i\sigma_j\sigma_k + ... \quad (1)$$

where H_0 is the background energy (the energy due to the graphene layer in our case), h_i is the singlet contribution (a single epoxide), J_{ij} and J_{ijk} are the pair and triplets ECI, S_L are the number of sites in the supercell. In Equation 1 the infinite summation was truncated at the triplets. In facts, it was proven in literature that, by properly truncating the expansion

at a finite amount of figures, it is possible to represent the configurational energy with good precision.[32] To find the figures and the ECIs, the total energy of some configurations must be provided. This is typically achieved by calculating the configurational energy by means of DFT simulations. The accuracy of the expansion depends on the amount of the ECIs taken into consideration and the training set to used extract them.[33] The predictive power of the expansion is represented by a parameter, called cross validation score which evaluates the difference between predicted and known energies for different sets of data. The main goal is to find the proper figures and ECIs that minimize the cross validation score below, at least, 0.025 eV and then to use these ECIs to quickly predict the energy of any configuration without recurring to other computational demanding DFT simulations (for a more detailed explanation of the method see Ref.[33]). CE was performed by means of the Alloys Theoretic Automated Toolkit (ATAT) software package[33] and the DFT calculation by means of the QUANTUM ESPRESSO program.[34] The expansion was trained selecting only structures with few epoxides in order to reliably describe the formation of small clusters. We calculated by means of DFT all the epoxides pairs and triplets up to a diameter of 6 Å and all the quadruplets up to 5 Å (see Method section for more details about the DFT calculations). The structures including a pair of nearest neighbour epoxides were excluded from the fitting due to the instability of this configuration; the epoxides evolve to second nearest neighbours. Epoxides were positioned only on one side of the GO sheet as no particular difference in energy is reported between pairs on the same side or on opposite sides of GO (see Fig. S1 of the Supporting Information). With such a fitting set, it was possible to achieve an expansion of 14 figures with a cross validation score of 0.002 eV. The selected figures and their relative ECIs are shown in Fig. S2 of the Supporting Information. Here we show only the two most stable pairs and triplets (Fig. 2).

From the pair interactions in Fig. S1 of the Supporting Information we understand that there is no particular drive for clusterization but rather two main optimal configurations for which the energy is particularly low. Beside these configurations, the energy profile is rather

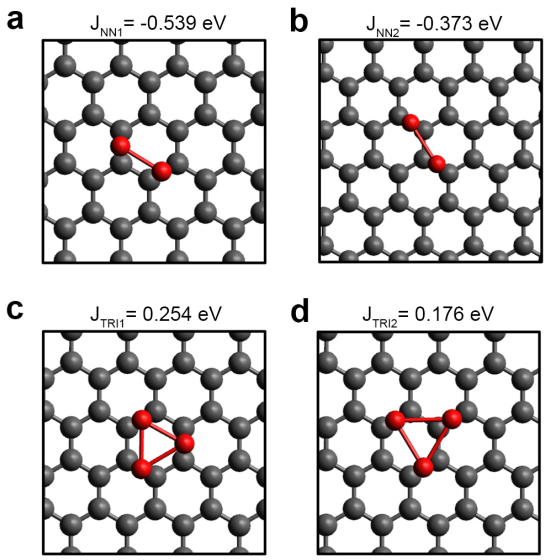

Figure 2: Most stable pair (a and b) and triplet (c and d) figures obtained with the CE and their related ECIs. A negative value indicates that the configuration lowers the total energy of the structure compared to the one composed by not-interacting epoxides, while a positive ECI corresponds to an increase in energy. The carbon atoms are represented in gray while the oxygen atoms in red.

flat, the interactions are therefore extremely short range. The two optimal arrangements also correspond to the lowest pair ECI configurations (Figs. 2a and 2b) that will play an important role in the dynamics of GO layers.

Concerning the triplets (Figs. 2c and 2d), although their ECIs are positive in energy because of the close distance among epoxides, the strong pair interaction is sufficient to make these triplet arrangements highly favourable. In facts, in CE the energy of a cluster is obtained considering all the contributions of the figures that form it. For instance, if we think the arrangement in Fig. 2c as a cluster of three epoxides and not as just a figure of the CE, its total energy is given by the sum of the energy of three singlets (h_i of Equation 1), the sum of the three pair ECIs in Fig. 2a (J_{NN1}) and the triplet ECI in Fig. 2c (J_{TRI1}). Clearly, a cluster maximizing the number of pairs shown in Fig. 2a and 2b is particularly stable and it will hardy lose an oxygen compared to a cluster having a random oxygen arrangement. The configuration dependent stability of the clusters given by the epoxide-epoxide interaction has important consequences on the dynamics of the functional groups on a GO layer as we will

show later in the text.

By knowing the configurational energy, it is possible to describe the evolution of the GO sheet in time. Both experiments and theoretical calculations suggest that over the course of a few days the GO layer undergoes a structural and chemical change due to modification of the distribution and of the amount of oxygen functional groups.[25,35] We computed the evolution of the GO sheet with KMC approach which simulates a sequence of events. The event occurring is randomly selected on the basis of its transition rate and the time is updated based on the sum of the rates. See Ref.[36,37] for a more detailed explanation of the KMC process. The simulations were carried out with the Zacros software.[31,38] We considered three main processes: the diffusion of epoxides, the desorption of two epoxides to form molecular oxygen and the adsorption and splitting of a molecular oxygen in two epoxides. All these processes are thermally activated and involve the overcoming of a potential barrier. The adsorbate-adsorbate interactions directly affect the rates at which the processes governing the evolution of a GO sheet take place. In practice, the barrier of a process in the zero-coverage limit, $E_{bar,0}$, can be higher or lower in presence of epoxides depending on the energy of the initial and final states, which are calculated by CE (see Supporting Information for more details). Given the energy barrier of a process it is possible to derive the related rate constant k as:

$$k = A \exp\left(- \frac{E_{bar}(\boldsymbol{\sigma})}{k_B T} \right) \tag{2}$$

Where $E_{bar}(\boldsymbol{\sigma})$ is the energy barrier considering epoxide-epoxide interactions, A is the pre-exponential factor, k_B is the Boltzmann constant and T is the temperature. Data on the zero-coverage limit barriers $E_{bar,0}$ and on the pre-exponential factor associated with the three processes (diffusion, adsorption, desorption) are shown in Table 1. The energy barriers are obtained by means of DFT calculations using the nudged elastic band algorithm while the pre-exponential factors are determined computing the phonon frequencies as indicated in Ref.[38] Data well agree with both experimental and theoretical results.[39]

Table 1: Forward potential barriers ($E_{bar,0}$) in the zero-coverage limit for epoxide diffusion, desorption (as O_2) and adsorption (from O_2 precursor) calculated by DFT simulations. A represents the corresponding pre-exponential factor estimated with DFT at 300 K and at an O_2 pressure of 1 bar.

	$E_{bar,0}$ (eV)	A (Hz)
Diffusion	0.76	6.4×10^{13}
Desorption	1.17	7.3×10^{13}
Adsorption	2.83	269

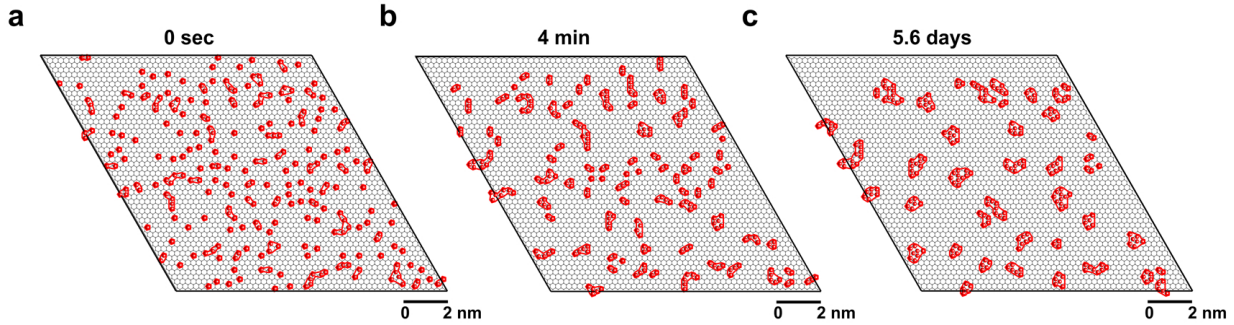

Figure 3: Evolution of a 5% GO layer at 300 K at different time: 0 second (a), 4 minutes (b), and 5.6 days (c). The red spheres indicate the epoxides; they are oversized for clarity with respect to the underlying graphene layer shown in a gray stick representation. The red lines outline the oxidized clustered areas.

Due to the high barrier and the low pre-exponential, the adsorption process is very unlikely to occur. For such a reason we considered only diffusion and desorption. We modeled the GO layer with a 120 x 120 $Å^2$ supercell. The aim of our study is to simulate the small metastable clusters occurring before the formation of separated GO and graphene areas. We investigated four coverages: a reduced GO with 5% coverage similarly to the one produced following the procedure of Hossain et al. and Bagri et al.,[27,40] two intermediate coverages of 10 and 15%, and a high coverage of 30% as a result of the typical Hummers method.[41] Two annealing temperatures were simulated, namely 300 and 350 K.

We first report the results of the simulation of a 5% GO layer exposed to a 300 K thermal process. Fig. 3a-c shows the dynamics of the functional group arrangement of a GO sample. The initial oxygen distribution was randomly generated, with only single epoxides present on GO monolayer (Fig. 3a). When isolated the epoxides are highly mobile and randomly diffuse

on the sheet, but in less than 4 minutes, they quickly come in contact (Fig. 3b) forming small clusters. We considered as belonging to the same clusters epoxides whose distance is below 4 Å. The newly formed clusters are highly metastable as they have random shapes. In order to decrease the energy of the system, they undergo a process of rearrangement in which the number of most stable pairs that we identified in Fig. 2 is maximized. During such a process the clusters can change their shape and diffuse. Eventually, they either coalesce with another cluster or they arrange into a lower energy configuration becoming immobile, pinned by the most stable figures. The clusterization process timescale is dictated by the environment-dependent diffusion barriers calculated at every step for each oxygen atom. The more stable the cluster, the lower is the energy of the arrangement, as calculated using CE. The diffusion barrier for the epoxide to detach will thus be higher than the one reported in Table 1 corresponding to the zero-coverage limit. Epoxides belonging to the stabilized clusters, then "oscillate" among almost isoenergetic positions. During the oscillation, one random epoxide can move farther and join another cluster. The latter process becomes more unlikely as the pristine graphene areas grow larger. In order to progress in the formation of larger clusters, the metastable equilibrium characterizing the pinned clusters must be locally broken so to allow the diffusion of part of their epoxides. For such reason the cluster enlargement is slow and even after 5 days (Fig. 3c) we can recognize some of the clusters formed after 4 minutes. The mean area of the oxidized clusters grew from 13 $Å^2$ to 31 $Å^2$ when passing from t = 4 minutes to t = 5.6 days meaning that the annealing time is an effective way to control the cluster size (the evolution of the cluster size distribution as a function of time is reported in the Supporting Information). The slowness of the clustering process is advantageous for industrial applications as there is a large time margin to stop the annealing when the desired size is achieved. The shape of the oxidized areas after the annealing process is quite circular: the calculated roundness of the clusters, defined as ratio between the perimeter and 4π times the area, has a mean value of 1.5 (close to the value of 1 which corresponds to a circle). During the simulation no desorption occurred suggesting

that such a process is highly improbable at room temperature. As such, the drive for the clustering is the energy minimization as consequence of structural rearrangement. Single epoxides, indeed, introduce highly energetic distortions in the graphene sheet due to the presence of irregular sp^3 bonds. When two or more epoxides come close the local stress is relieved, as demonstrated in literature[42] and by the values of the ECIs reported in this work. Ideally, the functional groups would tend to cluster all together, as a closely packed as possible, to form an oxidized island leaving pristine graphene behind. In the low coverage limit, however, since the distance between functional group is very large, direct formation of a single large island is impaired as small clusters composed by few oxygen atoms are sufficiently stable to prevent epoxide detachment (the stability of a few representative clusters is shown in the Supporting Information). As consequence, there is poor supply of epoxides for the expansion of the largest clusters resulting in a particularly slow growth process. Even after 5 days, the structure is still in a metastable state and it shows no sign of a dominating cluster type. The key to precisely control pore dimensions is the long time needed for clusters to grow. The slowness of the process enables one to interrupt the annealing without risking of overextending the clustering process which would results in membranes with oversize holes.

The increase in temperature from 300 K to 350 K has no effect on the mechanism of cluster formation nor on the tendency to desorb molecular oxygen. However, a remarkable speed up in the $-O-$ clustering is observed. For instance to give rise to an average area of the oxidized clusters of 31 $Å^2$ it takes 3.6 days at 300 K and 14 minutes at 350 K. This faster clusterization process predicted by our simulation at 350 K is consistent with experiments showing that annealing at 320-350 K originates two separated phases (pristine and oxidized) after several days.[13]

In case of higher coverages, we observe a progressive loss of roundness of the oxidized areas changing from 1.5 at 5% oxygen coverage to 1.8 at 10%, to 2.6 at 15% after 2 days of annealing (see the Supporting Information for the Figures of the post-annealing GO layers at 5, 10, 15 and 30% and the related cluster size distribution). In general, clusters at high

coverages tend to evolve into more linear configurations favoring the distribution of epoxides along zig-zag chains. For a coverage of 30% the identification of clusters becomes impossible because the oxidized areas are interconnected and therefore they extend over the entire simulation supercell. The high coverage layers are likely to quickly yield to separated large pristine and oxidized graphene areas.

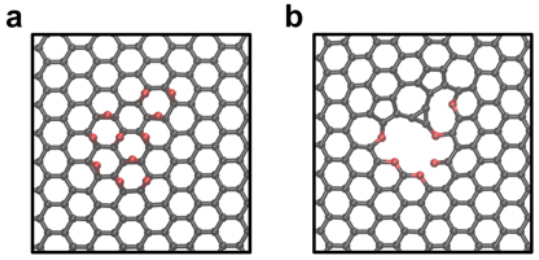

Figure 4: Example of oxidized GO cluster before (a) and after (b) the high temperature reducing treatment.

Once a sheet presenting clustered oxidized areas was obtained, we simulated the impact of a more intense thermal treatment. Several thermal processes for both graphene and GO were studied in literature.[43–45] Among them, the high temperature reducing process[12,46] differs from the microwave reduction[47] as it targets the entire sheet rather than only the epoxide bonds. As a consequence, the former effectively causes carbon removal along with functional group desorption, while the latter is expected to favor oxygen desorption. For the purpose of creating pores in GO, we simulated a high temperature reducing treatment. To understand the effects of a harsh reducing process on clustered GO layers, we selected some of the clusters obtained from KMC and performed high temperature reactive[48] MD simulations by means of the LAMMPS software package (see Method section for more details).[49] An example of the effects of the reducing process is shown in Fig. 4a-b, where we performed the high temperature treatment on a clustered structure at 5% coverage resulting from 5 days of mild thermal annealing at 300 K. The area of the final pore is 24.3 $Å^2$ comparable with the critical area required to filter salt (23.8 $Å^2$).[2] During annealing only CO and CO_2 molecules are extracted from the GO sheet in agreement with the mechanism proposed by Larciprete

et al. for the formation of vacancies in GO. In general, only clustered oxidized areas give rise to carbon removal and to pores whose edges are often saturated by ether groups. *Ab initio* molecular dynamics tests confirmed that carbon desorbs from graphene oxide clusters as CO or CO_2 molecules at high temperature. The pristine graphene surrounding the cluster, on the contrary, is not damaged by the treatment. As a result, the pores dimensions are directly related to the size of the initial oxidized areas so that controlling the clusterization process is a means to tune the final pore size. The formation of pores suited for desalination appear to be harder for larger coverages, since an increase in epoxide amount leads to linear shaped clusters or interconnected oxidized regions. To show how decisive is the effect of slow clustering, we performed similar calculations on some of the configurations obtained after 4 minutes of annealing (see Supporting Information). Although the GO layer is damaged by the thermal reducing process, the resulting pores are not large enough to let water molecules pass. It is then important, before exposing GO to a high temperature process, to let the functional groups cluster long enough to produce larger oxidized regions.

To summarize, we proposed a scalable method to consistently generate pores of controlled dimensions based on results obtained by means of a combination of theoretical simulations such as molecular dynamics, DFT, Cluster Expansion and KMC. Starting from an as-grown GO layer at low coverage ($\leq$10%), with epoxides randomly distributed on the graphene basal plane, the monolayer is treated with a mild annealing process at fixed low temperature (300-320 K) so that its -O- groups are allowed to cluster. At these temperatures the clustering is slow, thus one can stop the process when the clusters are of the required dimension for the desired application. After that, GO is annealed at high temperature, causing the desorption of epoxides along with part of the carbon atoms only in the oxidized regions, while pristine graphene areas remain unaltered. Pores, whose area is proportional to the oxidized area, are then produced only in the clustered regions. Such a scalable procedure opens up to the possibility to realize graphene membranes for desalination at the industrial level.

Acknowledgement

We acknowledge the CINECA award under the ISCRA initiative and HPC@POLITO for the availability of high-performance computing resources and support. This work is part of the "DESAL" project funded by Politecnico di Torino. The authors declare no competing financial interests.

Supporting Information

Pair interaction on graphene sheet, cluster expansion figures, coverage dependent barrier, cluster size density evolution over time, coverage effect, diffusion barrier variation, reducing process effects on an early clustered GO layer, molecular dynamics method, Density Functional Theory method.

References

(1) Subramani, A.; Jacangelo, J. G. Emerging desalination technologies for water treatment: a critical review. *Water Res.* **2015**, *75*, 164–187.

(2) Cohen-Tanugi, D.; Grossman, J. C. Water desalination across nanoporous graphene. *Nano Lett.* **2012**, *12*, 3602–3608.

(3) Konatham, D.; Yu, J.; Ho, T. A.; Striolo, A. Simulation insights for graphene-based water desalination membranes. *Langmuir* **2013**, *29*, 11884–11897.

(4) Cohen-Tanugi, D.; McGovern, R. K.; Dave, S. H.; Lienhard, J. H.; Grossman, J. C. Quantifying the potential of ultra-permeable membranes for water desalination. *Energy Environ. Sci.* **2014**, *7*, 1134–1141.

(5) Fischbein, M. D.; Drndićć, M. Electron beam nanosculpting of suspended graphene sheets. *Appl. Phys. Lett.* **2008**, *93*, 113107.

(6) Clochard, M.-C.; Melilli, G.; Rizza, G.; Madon, B.; Alves, M.; Wegrowe, J.-E.; Toimil-Molares, M.-E.; Christian, M.; Ortolani, L.; Rizzoli, R. et al. Large area fabrication of self-standing nanoporous graphene-on-PMMA substrate. *Mater. Lett.* **2016**, *184*, 47–51.

(7) Russo, C. J.; Golovchenko, J. A. Atom-by-atom nucleation and growth of graphene nanopores. *Proc. Natl. Acad. Sci.* **2012**, *109*, 5953–5957.

(8) Surwade, S. P.; Smirnov, S. N.; Vlassiouk, I. V.; Unocic, R. R.; Veith, G. M.; Dai, S.; Mahurin, S. M. Water desalination using nanoporous single-layer graphene. *Nat. Nanotechnol.* **2015**, *10*, 459–464.

(9) Koenig, S. P.; Wang, L.; Pellegrino, J.; Bunch, J. S. Selective molecular sieving through porous graphene. *Nat. Nanotechnol.* **2012**, *7*, 728–732.

(10) Bai, Z.; Zhang, L.; Li, H.; Liu, L. Nanopore creation in graphene by ion beam irradiation: geometry, quality, and efficiency. *ACS Appl. Mater. Interfaces* **2016**, *8*, 24803–24809.

(11) Savazzi, F.; Risplendi, F.; Mallia, G.; Harrison, N. M.; Cicero, G. Unravelling some of the structure-property relationships in graphene oxide at low degree of oxidation. *J. Phys. Chem. Lett.* **2018**, *9*, 1746–1749.

(12) Lin, L.-C.; Grossman, J. C. Atomistic understandings of reduced graphene oxide as an ultrathin-film nanoporous membrane for separations. *Nat. Commun.* **2015**, *6*, 8335.

(13) Kumar, P. V.; Bardhan, N. M.; Tongay, S.; Wu, J.; Belcher, A. M.; Grossman, J. C. Scalable enhancement of graphene oxide properties by thermally driven phase transformation. *Nat. Chem.* **2014**, *6*, 151–158.

(14) Kumar, P. V.; Bardhan, N. M.; Chen, G.-Y.; Li, Z.; Belcher, A. M.; Grossman, J. C.

New insights into the thermal reduction of graphene oxide: impact of oxygen clustering. *Carbon* **2016**, *100*, 90–98.

(15) Lee, Y. K.; Choi, H.; Lee, C.; Lee, H.; Goddeti, K. C.; Moon, S. Y.; Doh, W. H.; Baik, J.; Kim, J.-S.; Choi, J. S. et al. Charge transport-driven selective oxidation of graphene. *Nanoscale* **2016**, *8*, 11494–11502.

(16) Park, W. K.; Yoon, Y.; Song, Y. H.; Choi, S. Y.; Kim, S.; Do, Y.; Lee, J.; Park, H.; Yoon, D. H.; Yang, W. S. High-efficiency exfoliation of large-area mono-layer graphene oxide with controlled dimension. *Sci. Rep.* **2017**, *7*, 16414.

(17) Eigler, S.; Enzelberger-Heim, M.; Grimm, S.; Hofmann, P.; Kroener, W.; Geworski, A.; Dotzer, C.; Rockert, M.; Xiao, J.; Papp, C. et al. Wet chemical synthesis of graphene. *Adv. Mater.* **2013**, *25*, 3583–3587.

(18) Vijayarangamuthu, K.; Ahn, S.; Seo, H.; Yoon, S.; Park, C.; Jeon, K. Temporospatial control of graphene wettability. *Adv. Mater.* **2016**, *28*, 661–667.

(19) Raffone, F.; Ataca, C.; Grossman, J. C.; Cicero, G. MoS2 enhanced T-phase stabilization and tunability through alloying. *J. Phys. Chem. Lett.* **2016**, *7*, 2304–2309.

(20) van de Walle, A.; Ellis, D. E. First-principles thermodynamics of coherent interfaces in samarium-doped ceria nanoscale superlattices. *Phys. Rev. Lett.* **2007**, *98*, 266101.

(21) Fuks, D.; Dorfman, S. Vacancy interactions in cluster expansion formalism. *Int. J. Quantum Chem.* **2001**, *85*, 301–306.

(22) Bajpai, A.; Frey, K.; Schneider, W. F. Binary approach to ternary cluster expansions: NO-O-vacancy system on Pt(111). *J. Phys. Chem. C* **2017**, *121*, 7344–7354.

(23) Piccinin, S.; Stamatakis, M. CO oxidation on Pd(111): a first-principles-based kinetic Monte Carlo study. *ACS Catal.* **2014**, *4*, 2143–2152.

(24) Bray, J. M.; Schneider, W. F. First-principles analysis of structure sensitivity in NO oxidation on Pt. *ACS Catal.* **2015**, *5*, 1087–1099.

(25) Zhou, S.; Bongiorno, A. Origin of the chemical and kinetic stability of graphene oxide. *Sci. Rep.* **2013**, *3*, 2484.

(26) Tararan, A.; Zobelli, A.; Benito, A. M.; Maser, W. K.; Stepḣan, O. Revisiting graphene oxide chemistry via spatially-resolved electron energy loss spectroscopy. *Chem. Mater.* **2016**, *28*, 3741–3748.

(27) Hossain, M. Z.; Johns, J. E.; Bevan, K. H.; Karmel, H. J.; Liang, Y. T.; Yoshimoto, S.; Mukai, K.; Koitaya, T.; Yoshinobu, J.; Kawai, M. et al. Chemically homogeneous and thermally reversible oxidation of epitaxial graphene. *Nat. Chem.* **2012**, *4*, 305–309.

(28) Chua, C. K.; Pumera, M. Selective removal of hydroxyl groups from graphene oxide. *Chem. Eur. J.* **2013**, *19*, 2005–2011.

(29) Xu, C.; Yuan, R.-S.; Wang, X. Selective reduction of graphene oxide. *New Carbon Mater.* **2014**, *29*, 61–66.

(30) Mathkar, A.; Tozier, D.; Cox, P.; Ong, P.; Galande, C.; Balakrishnan, K.; Reddy, A. L. M.; Ajayan, P. M. Controlled, stepwise reduction and band gap manipulation of graphene oxide. *J. Phys. Chem. Lett.* **2012**, *3*, 986.

(31) Nielsen, J.; d'Avezac, M.; Hetherington, J.; Stamatakis, M. Parallel kinetic Monte Carlo simulation framework incorporating accurate models of adsorbate lateral interactions. *J. Chem. Phys.* **2013**, *139*, 224706.

(32) Connolly, J. W. D.; Williams, A. R. Density-functional theory applied to phase transformations in transition-metal alloys. *Phys. Rev. B* **1983**, *27*, 5169.

(33) van de Walle, A.; Ceder, G. Automating first-principles phase diagram calculations. *J. Phase Equilib.* **2002**, *23*, 348.

(34) Giannozzi, P.; Baroni, S.; Bonini, N.; Calandra, M.; Car, R.; Cavazzoni, C.; Ceresoli, D.; Chiarotti, G. L.; Cococcioni, M.; Dabo, I. et al. QUANTUM ESPRESSO: a modular and open-source software project for quantum simulations of materials.

(35) Kim, S.; Zhou, S.; Hu, Y.; Acik, M.; Chabal, Y. J.; Berger, C.; de Heer, W.; Bongiorno, A.; Riedo, E. Room-temperature metastability of multilayer graphene oxide films. *Nat. Mater.* **2012**, *11*, 544–549.

(36) Jansen, A. P. J. *An introduction to kinetic Monte Carlo simulations of surface reactions*; Springer: Berlin, Germany, 2012.

(37) Raffone, F.; Cicero, G. Unveiling the fundamental role of temperature in RRAM switching mechanism by multiscale simulations. *ACS Appl. Mater. Interfaces* **2018**, *10*, 7512–7519.

(38) Stamatakis, M.; Vlachos, D. G. A graph-theoretical kinetic Monte Carlo framework for on-lattice chemical kinetics. *J. Chem. Phys.* **2011**, *134*, 214115.

(39) Larciprete, R.; Fabris, S.; Sun, T.; Lacovig, P.; Baraldi, A.; Lizzit, S. Dual path mechanism in the thermal reduction of graphene oxide. *J. Am. Chem. Soc.* **2011**, *133*, 17315–17321.

(40) Bagri, A.; Mattevi, C.; Acik, M.; Chabal, Y. J.; Chhowalla, M.; Shenoy, V. B. Structural evolution during the reduction of chemically derived graphene oxide. *Nat. Chem.* **2010**, *2*, 581–587.

(41) Hummers, W. S.; Offeman, R. E. Preparation of graphitic oxide. *J. Am. Chem. Soc.* **1958**, *80*, 1339.

(42) Li, J.-L.; Kudin, K. N.; McAllister, M. J.; Prudhomme, R. K.; Aksay, I. A.; Car, R. Oxygen-driven unzipping of graphitic materials. *Phys. Rev. Lett.* **2006**, *96*, 176101.

(43) Xu, Z.; Ao, Z.; Chu, D.; Younis, A.; Li, C. M.; Li, S. Reversible hydrophobic to hydrophilic transition in graphene via water splitting induced by UV irradiation. *Sci. Rep.* **2014**, *4*, 6450.

(44) Botas, C.; Alvarez, P.; Blanco, C.; Santamaria, R.; Granda, M.; Gutierrez, M. D.; Rodriguez-Reinoso, F.; Menendez, R. Critical temperatures in the synthesis of graphene-like materials by thermal exfoliation-reduction of graphite oxide. *Carbon* **2013**, *52*, 476–485.

(45) Garino, N.; Sacco, A.; Castellino, M.; Munoz-Tabares, J. A.; Chiodoni, A.; Agostino, V.; Margaria, V.; Gerosa, M.; Massaglia, G.; Quaglio, M. Microwave-assisted synthesis of reduced graphene oxide/SnO_2 nanocomposite for oxygen reduction reaction in microbial fuel cells. *ACS Appl. Mater. Interfaces* **2016**, *8*, 4633–4643.

(46) Shin, D. S.; Kim, H. G.; Ahn, H. S.; Jeong, H. Y.; Kim, Y.-J.; Odkhuu, D.; Tsogbadrakh, N.; Lee, H.-B.-R.; Kim, B. H. Distribution of oxygen functional groups of graphene oxide obtained from low-temperature atomic layer deposition of titanium oxide. *RCS Adv.* **2017**, *7*, 13979–13984.

(47) Voiry, D.; Yang, J.; Kupferberg, J.; Fullon, R.; Lee, C.; Jeong, H. Y.; Shin, H. S.; Chhowalla, M. High-quality graphene via microwave reduction of solution-exfoliated graphene oxide. *Science* **2016**, *353*, 1413–1416.

(48) Chenoweth, K.; van Duin, A. C.; Goddard, W. A. ReaxFF reactive force field for molecular dynamics simulations of hydrocarbon oxidation. *J. Phys. Chem. A* **2008**, *112*, 1040–1053.

(49) Plimpton, S. Fast parallel algorithms for short-range molecular dynamics. *J. Comput. Phys.* **1995**, *117*, 1–19.